

Backstepping control with energy reduction for an over-actuated marine platform

Aristomenis Tsopelakos, *Student Member, IEEE*, Kostas Vlachos, and
 Evangelos Papadopoulos, *Senior Member, IEEE*

Abstract— We present the design of a backstepping controller for a triangular over-actuated marine platform, controlled by three rotating jets. Our goal is the stabilization of the position and the orientation of the platform, under realistic environmental disturbances, such as wind forces, wave forces and hydrodynamic forces. Actuator thrust and angle dynamics, as well as settling delays, in the rotation of the jets and in the response of the desired thrust, are included in the algorithm, despite the presence of an allocation scheme. Thrust and angle velocity, limitations are also taken into account. A Thrust Upper Limit (TUL) manipulation heuristic is introduced in order to reduce the thrust requirements and the energy consumed. The performance of the developed backstepping controller is compared to the case with and without the TUL. Simulation results show that the use of the heuristic reduces energy consumption.

I. INTRODUCTION

Floating platforms are used for the construction of underwater structures. Our platform “Vereniki”, see Fig. 1, was designed to assist in the deployment of the deep-sea neutrino telescope “Nestor”, [1]. These platforms must be kept inside a predefined area. To this end, they are equipped with actuation systems that provide the necessary dynamic positioning forces, see [2], [3], [4]. They are over-actuated, for fault tolerance reasons and for advanced maneuver capabilities. As a result, the application of an appropriate allocation scheme is necessary. An extended study on control allocation is presented in [5].

Floating platform dynamics are inherently nonlinear and as a result, nonlinear control techniques must be adopted for their positioning. Backstepping controllers have been proposed in the past mainly for tracking control of ships [6-7], and the control of under-actuated surface vessels [8] and under-actuated AUVs [9]. A study on the properties of backstepping for marine vehicles is presented in [10]. The tracking control of a highly over-actuated system is proposed in [11]. The dynamic model of the platform, a model-based controller and an allocation scheme were proposed in [12], and a linear MPC controller in [13]. In the bibliography, actuator dynamics and settling time are considered as a kind of disturbance and are omitted from the control analysis.

In this paper, we include the dynamics in thrust response and in the jets angle response, as well as the limitations in jet thrusts and jet angular velocities, [14]. The dynamics of the

thrusts and the angles are included in the backstepping algorithm, assuming that the development of the forces and the torque on the center mass (CM) of the platform is also governed by specific dynamics. This assumption cannot be supported in the design of a model-based controller, because the forces/torque are used as control inputs for the cancellation of nonlinearities to yield a linear system.

The developed backstepping controller is robust in errors in mass estimation; an important property for platforms which carry massive objects. The asymptotic stability of the final system is established using the comparison lemma on a Lyapunov function. To reduce the energy consumption, the thrust upper limit manipulation heuristic, called here (TUL), is introduced. Simulation results, including realistic environmental disturbances validate the robustness of the controllers and the effectiveness of the heuristic.

II. DESCRIPTION OF THE PLATFORM “VERENIKI”

“Vereniki” is an isosceles platform governed by three rotating diesel engine jets. “Vereniki” has three hollow double-cylinders, one at each corner of the platform, which provide the necessary buoyancy. They contain the pump-jets, the diesel engines and the electro-hydraulic motors that rotate jets. The rotation of the jets is parallel to the sea surface, thrust limit is 20kN. The settling time in the jet *thrust* response is about 4 s and in the jet *angle* response is about 5 s. The jet angular velocity limit is 0.84 rad/s. The platform position/orientation are obtained by GPS, [12].

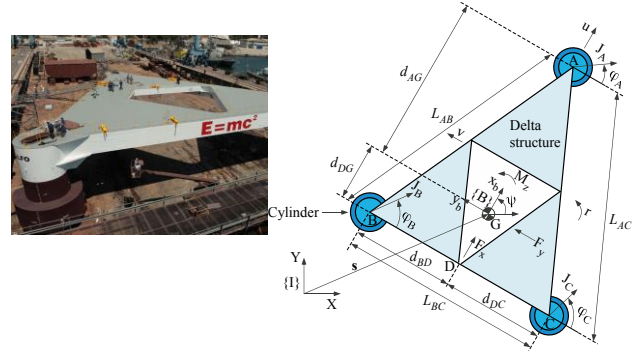


Figure 1. The platform Vereniki, and its 2D graphical representation.

A. Kinematics

The kinematics equation for the planar motion of the platform is given by (1). In (1), x and y represent the platform CM inertial coordinates and ψ describes the orientation of the body-fixed frame {B}, whose origin is at the platform CM, see Fig. 1; u and v are the surge and sway

A. Tsopelakos (e-mail: tsopelakosaris121@yahoo.gr), and E. Papadopoulos (egpapado@central.ntua.gr) are with the Department of Mechanical Engineering, National Technical University of Athens, 15780 Athens, Greece. Kostas Vlachos is with the Department of Computer Science & Engineering, University of Ioannina (kostaswl@cs.uoi.gr).

velocities respectively, defined in the body-fixed frame $\{B\}$, and r is the yaw (angular) velocity of the platform, with $s \cdot = \sin(\cdot)$, and $c \cdot = \cos(\cdot)$.

$$\begin{bmatrix} \dot{x} \\ \dot{y} \\ \dot{\psi} \end{bmatrix} = \begin{bmatrix} c\psi & -s\psi & 0 \\ s\psi & c\psi & 0 \\ 0 & 0 & 1 \end{bmatrix} \begin{bmatrix} u \\ v \\ r \end{bmatrix} \Rightarrow {}^I \dot{\mathbf{x}} = {}^I \mathbf{J}_B {}^B \mathbf{v} \quad (1)$$

B. Dynamics

1) Control forces/ torque

The J_A , J_B , and J_C in Fig. 1 denote the magnitude of the thrusts, while the angles φ_A , φ_B , and φ_C denote the force directions. These thrusts provide control resultant forces along the x_b and y_b axes, the $F_{c,x}$ and $F_{c,y}$ respectively acting at the CM, and a torque $N_{c,z}$ about z_b , according to:

$${}^B \boldsymbol{\tau}_c = [F_{c,x}, F_{c,y}, N_{c,z}]^T = \mathbf{B} {}^B \mathbf{f}_c \quad (2a)$$

$$\mathbf{B} = \begin{bmatrix} 1 & 0 & 0 \\ 0 & -1 & -d_{AG} \\ 1 & 0 & -d_{DC} \\ 0 & -1 & d_{DG} \\ 1 & 0 & d_{DC} \\ 0 & -1 & d_{DG} \end{bmatrix}^T, \quad {}^B \mathbf{f}_c = \begin{bmatrix} J_A s \varphi_A \\ J_A c \varphi_A \\ J_B s \varphi_B \\ J_B c \varphi_B \\ J_C s \varphi_C \\ J_C c \varphi_C \end{bmatrix} \quad (2b)$$

$$J_i = \sqrt{(J_i s \varphi_i)^2 + (J_i c \varphi_i)^2}, \quad \varphi_i = a \tan 2(J_i s \varphi_i, J_i c \varphi_i) \quad (3)$$

where $i = A, B, C$, ${}^B \boldsymbol{\tau}_c$ is the control force/ torque vector, and the dimensional parameters in \mathbf{B} are defined in Fig. 1. After the computation of the desired control forces/torque, the desired thrusts and angles, can be retrieved by the pseudo-inversion of \mathbf{B} in (2a) together with (3), see [12].

2) Hydrodynamic forces and environmental disturbances

The hydrodynamic force acting on the platform CM is represented by vector ${}^B \mathbf{q}$:

$${}^B \mathbf{q} = [f_x, f_y, n_z]^T \quad (4)$$

For an analysis of the hydrodynamic forces acting on the platform CM, see [2], [4]. The disturbance vector ${}^B \mathbf{q}_{dist}$, represents wind and wave generated forces and torques, see Fig. 4. Maximum disturbance values are derived from meteorological data collected from [1]. For the simulation models for wind, waves forces/torque see [4], [12].

We assume that the CM of the platform is at the triangle centroid and that the angular rate of the platform and as such of the reference frame is so low that it can be neglected. We derive the planar equations of motion, in $\{B\}$:

$$\mathbf{M} {}^B \dot{\mathbf{v}} = {}^B \mathbf{q} + {}^B \mathbf{q}_{dist} + {}^B \boldsymbol{\tau}_c \quad (5a)$$

$$\mathbf{M} = \begin{bmatrix} m - 3m_a & 0 & 0 \\ 0 & m - 3m_a & 0 \\ 0 & 0 & m_{33} \end{bmatrix} \quad (5b)$$

$$m_{33} = I_{zz} - (d_{AG}^2 + 2d_{BD}^2 + 2d_{DG}^2)m_a$$

where m is the mass of the platform, m_a is its added mass, and I_{zz} is its mass moment of inertia about the z_b axis. A detailed description of kinematics, dynamics and the computation of matrix \mathbf{M} can be found in [12].

3) Actuator dynamics

The jet thrust, and rotation dynamics responses correspond to first order systems, based on data provided by the jets manufacturer, are:

$$\begin{aligned} \dot{J}_i &= (1/\tau_j)(J_{i,des} - J_i) \\ \dot{\varphi}_i &= (1/\tau_\varphi)(\varphi_{i,des} - \varphi_i) \end{aligned} \quad (i=A, B, C) \quad (6)$$

where τ_φ and τ_j are the jet thrust, and rotation time constant.

The control forces/ torque vector ${}^B \boldsymbol{\tau}_c$ is due to jet vectored thrust whose dynamics is described by first order systems, given by (6). Consequently, the forces/ torque acting on the CM of the platform, can be approximated by the response of a first order system, see (7a),

$${}^B \dot{\boldsymbol{\tau}}_c = -(1/\tau_1) {}^B \boldsymbol{\tau}_c + (1/\tau_1) {}^B \boldsymbol{\tau}_{c,des} \quad (7a)$$

However, ${}^B \mathbf{f}_c$ contains multiplications of the thrust with the sine or cosine of the angles, which renders the allocation scheme a non-linear transformation. This fact suggests the use of a higher order system for the approximation of the response of the forces/ torque acting on the CM of the platform. For the second order system see (7b).

$${}^B \dot{\boldsymbol{\tau}}_c = -(1/\tau_2) {}^B \dot{\boldsymbol{\tau}}_c - (1/\tau_2) {}^B \boldsymbol{\tau}_c + (1/\tau_2) {}^B \boldsymbol{\tau}_{c,des} \quad (7b)$$

where τ_1 and τ_2 are the actuator dynamics time constants for the first and the second order system respectively, and ${}^B \boldsymbol{\tau}_{c,des}$ represents the desired control inputs, given by,

$${}^B \boldsymbol{\tau}_{c,des} = [u_{F_{c,x}}, u_{F_{c,y}}, u_{N_{c,z}}]^T \quad (7c)$$

III. DESIGN OF THE BACKSTEPPING CONTROLLER

The system under control is governed by equations (1), (5) and (7) which are grouped together in (8). Equation (5) is included in the design of the controller without the term ${}^B \mathbf{q}_{dist}$, which is treated as an external disturbance. The use of a first order system for the approximation of the dynamics of forces/torque will be denoted as **case A**, while the use of a second order system **case B**, respectively.

$${}^I \dot{\mathbf{x}} = {}^I \mathbf{J}_B {}^B \mathbf{v} \quad (8a)$$

$${}^B \dot{\mathbf{v}} = \mathbf{M}^{-1} ({}^B \mathbf{q} + {}^B \boldsymbol{\tau}_c) \quad (8b)$$

$${}^B \dot{\boldsymbol{\tau}}_c = -(1/\tau_1) {}^B \boldsymbol{\tau}_c + (1/\tau_1) {}^B \boldsymbol{\tau}_{c,des} \quad (8c)$$

or

$${}^B \dot{\boldsymbol{\tau}}_c = -(1/\tau_2) {}^B \dot{\boldsymbol{\tau}}_c - (1/\tau_2) {}^B \boldsymbol{\tau}_c + (1/\tau_2) {}^B \boldsymbol{\tau}_{c,des} \quad (8d)$$

The nonlinear differential equations that govern the positioning are in strict-feedback form, [15]. The reference position, direction and velocities are: $x_R, y_R, \psi_R, u_R, v_R$, and r_R respectively. The tracking errors are defined as $x_e = x - x_R, y_e = y - y_R, \psi_e = \psi - \psi_R, u_e = u - u_R, v_e = v - v_R$, and $r_e = r - r_R$.

A. Preliminary Manipulation

Using the definition of the tracking errors, and after substitution of x, y, ψ, u, v, r in (1), we take the following position error equation presented in (9). Since u_R , and v_R are bounded desired linear velocities, the quantities δ_1 and δ_2 are considered also bounded quantities due to (9c). In addition, for a stabilized ψ ($\psi \rightarrow \psi_R$), the disturbance is close to zero.

$$\begin{bmatrix} \dot{x}_e \\ \dot{y}_e \end{bmatrix} = \begin{bmatrix} c\psi & -s\psi \\ s\psi & c\psi \end{bmatrix} \begin{bmatrix} u_e \\ v_e \end{bmatrix} + \begin{bmatrix} \delta_1 \\ \delta_2 \end{bmatrix} \quad (9a)$$

$$\dot{\psi}_e = r_e \quad (9b)$$

$$\delta = \begin{bmatrix} \delta_1 \\ \delta_2 \end{bmatrix} = \begin{bmatrix} c\psi - c\psi_R & -s\psi + s\psi_R \\ s\psi - s\psi_R & c\psi - c\psi_R \end{bmatrix} \begin{bmatrix} u_R \\ v_R \end{bmatrix} \quad (9c)$$

B. The Stabilization Process - case A

Our goal is to stabilize the platform position and orientation error to zero. We are setting up a Lyapunov function.

1) Step 1

For the stabilization of subsystem (9a), we select as virtual controls, the variables u_e and v_e . We are choosing the following Lyapunov function:

$$V_1 = (1/2)x_e^2 + (1/2)y_e^2 \quad (10)$$

The desired values for u_e, v_e are:

$$\begin{bmatrix} u_{e,des} \\ v_{e,des} \end{bmatrix} = - \begin{bmatrix} c\psi & s\psi \\ -s\psi & c\psi \end{bmatrix} [\mathbf{K} + \mathbf{K}_1] \begin{bmatrix} x_e \\ y_e \end{bmatrix} \quad (11)$$

$$\mathbf{K} = \text{diag}(k, k), \quad \mathbf{K}_1 = \text{diag}(k_1, k_1)$$

where k, k_1 are positive numbers. The substitution of these desired values in (9a), yields an exponentially decreasing relation augmented by bounded disturbances. This relation reassures convergence to a neighborhood of (0,0):

$$\begin{bmatrix} \dot{x}_e \\ \dot{y}_e \end{bmatrix} = - \begin{bmatrix} k+k_1 & 0 \\ 0 & k+k_1 \end{bmatrix} \begin{bmatrix} x_e \\ y_e \end{bmatrix} + \begin{bmatrix} \delta_1 \\ \delta_2 \end{bmatrix} \quad (12)$$

The time derivative of V_1 becomes:

$$\dot{V}_1 = -kx_e^2 - ky_e^2 - k_1(x_e - \frac{\delta_1}{2k_1})^2 - k_1(y_e - \frac{\delta_2}{2k_1})^2 + \frac{\|\delta\|^2}{4k_1} \quad (13)$$

Both k, k_1 are necessary to formulate the quadratic form (13). By choosing a large k_1 , the term $\|\delta\|^2/4k_1$ can be very small. Since, u_e , and v_e are virtual controls, we introduce the following error variables and stabilize them to (0,0):

$$z_u = u_e - u_{e,des} \Rightarrow u_e = z_u + u_{e,des} \quad (14)$$

$$z_v = v_e - v_{e,des} \Rightarrow v_e = z_v + v_{e,des}$$

Using (11), and (14) we substitute u_e and v_e in (9) and yields:

$$\begin{bmatrix} \dot{x}_e \\ \dot{y}_e \end{bmatrix} = - \begin{bmatrix} k+k_1 & 0 \\ 0 & k+k_1 \end{bmatrix} \begin{bmatrix} x_e \\ y_e \end{bmatrix} + \begin{bmatrix} c\psi & -s\psi \\ s\psi & c\psi \end{bmatrix} \begin{bmatrix} z_u \\ z_v \end{bmatrix} + \begin{bmatrix} \delta_1 \\ \delta_2 \end{bmatrix} \quad (15)$$

Using (11) and (9a) we compute the derivatives $u_{e,des}, v_{e,des}$.

$$\dot{u}_{e,des} = -(k+k_1)u_e - (k+k_1)(\delta_1 c\psi + \delta_2 s\psi) \quad (16)$$

$$\dot{v}_{e,des} = -(k+k_1)v_e - (k+k_1)(-\delta_1 s\psi + \delta_2 c\psi)$$

From (8b), the time derivatives of the velocity errors are:

$$\dot{u}_e = (1/(m-3m_a))(f_x + F_{c,x}) - \dot{u}_R \quad (17)$$

$$\dot{v}_e = (1/(m-3m_a))(f_y + F_{c,y}) - \dot{v}_R$$

and using (14), (16), and (17) the differential equations of the error variables are found to be,

$$\begin{aligned} \dot{z}_u &= (1/(m-3m_a))f_x - \dot{u}_R + (k+k_1)u_e \\ &\quad + (k+k_1)(\delta_1 c\psi + \delta_2 s\psi) + (1/(m-3m_a))F_{c,x} \\ \dot{z}_v &= (1/(m-3m_a))f_y - \dot{v}_R + (k+k_1)v_e \\ &\quad - (k+k_1)(\delta_1 s\psi - \delta_2 c\psi) + (1/(m-3m_a))F_{c,y} \end{aligned} \quad (18)$$

2) Step 2

We stabilize (18) to (0,0). Forces $F_{c,x}$, and $F_{c,y}$ are considered virtual controls. The Lyapunov function, and its time derivative are given below. After the introduction of errors z_u, z_v , the derivatives of x_e and y_e are given by (15).

$$V_2 = (1/2)(x_e^2 + y_e^2 + z_u^2 + z_v^2) \quad (19)$$

$$\begin{aligned} \dot{V}_2 &= \dot{V}_1 + z_u((1/(m-3m_a))f_x - \dot{u}_R + (k+k_1)u_e \\ &\quad + (k+k_1)(\delta_1 c\psi + \delta_2 s\psi) + (x_e c\psi + y_e s\psi) \\ &\quad + (1/(m-3m_a))F_{c,x}) + z_v((1/(m-3m_a))f_y - \dot{v}_R \\ &\quad + (k+k_1)v_e - (k+k_1)(\delta_1 s\psi - \delta_2 c\psi) \\ &\quad + (-x_e s\psi + y_e c\psi) + (1/(m-3m_a))F_{c,y}) \end{aligned} \quad (20)$$

Setting the desired values

$$\begin{aligned} F_{c,x,des} &= (m-3m_a)(-(1/(m-3m_a))f_x + \dot{u}_R \\ &\quad - (k+k_1)u_e - (k+k_1)(\delta_1 c\psi + \delta_2 s\psi) \\ &\quad - (x_e c\psi + y_e s\psi) - c_u z_u) \end{aligned} \quad (21)$$

$$\begin{aligned} F_{c,y,des} &= (m-3m_a)(-(1/(m-3m_a))f_y + \dot{v}_R \\ &\quad - (k+k_1)v_e + (k+k_1)(\delta_1 s\psi - \delta_2 c\psi) \\ &\quad - (-x_e s\psi + y_e c\psi) - c_v z_v) \end{aligned}$$

the time derivative of V_2 becomes

$$\dot{V}_2 = \dot{V}_1 - c_u z_u^2 - c_v z_v^2 \quad (22)$$

3) Step 3

The forces $F_{c,x}, F_{c,y}$ are not true controls, we have to introduce the following errors and stabilize them to (0,0):

$$z_{F_{c,x}} = F_{c,x} - F_{c,x,des} \Rightarrow F_{c,x} = z_{F_{c,x}} + F_{c,x,des} \quad (23)$$

$$z_{F_{c,y}} = F_{c,y} - F_{c,y,des} \Rightarrow F_{c,y} = z_{F_{c,y}} + F_{c,y,des}$$

After substitution of $F_{c,x}$, and $F_{c,y}$ in (18), we have the following subsystem:

$$\dot{z}_u = -c_u z_u - (x_e c\psi + y_e s\psi) + (1/(m-3m_a))z_{F_{c,x}} \quad (24)$$

$$\dot{z}_v = -c_v z_v - (-x_e s\psi + y_e c\psi) + (1/(m-3m_a))z_{F_{c,y}}$$

and using (8c) and (23) we have the following subsystem to be stabilized to zero,

$$\dot{z}_{F_{c,x}} = -(1/\tau_1)F_{c,x} - \dot{F}_{c,x,des} + (1/\tau_1)u_{F_{c,x}} \quad (25)$$

$$\dot{z}_{F_{c,y}} = -(1/\tau_1)F_{c,y} - \dot{F}_{c,y,des} + (1/\tau_1)u_{F_{c,y}}$$

We choose a new Lyapunov function:

$$V_3 = V_2 + (1/2)(z_{F_{c,x}}^2 + z_{F_{c,y}}^2) \quad (26)$$

and its derivative is

$$\begin{aligned} \dot{V}_3 &= \dot{V}_2 + z_{F_{c,x}}((1/(m-3m_a))z_u - \tau_1^{-1}F_{c,x} - \dot{F}_{c,x,des} \\ &\quad + \tau_1^{-1}u_{F_{c,x}}) + z_{F_{c,y}}((1/(m-3m_a))z_v \\ &\quad - \tau_1^{-1}F_{c,y} - \dot{F}_{c,y,des} + \tau_1^{-1}u_{F_{c,y}}) \end{aligned} \quad (27)$$

where all terms must be negative except the term $\|\delta\|^2/4k_I$. To this end, the true controls $u_{F_{c,x}}$, and $u_{F_{c,y}}$ are selected as:

$$\begin{aligned} u_{F_{c,x}} &= \tau_1(-m-3m_a)^{-1}z_u + \tau_1^{-1}F_{c,x} + \dot{F}_{c,x,des} - c_{F_{c,x}}z_{F_{c,x}} \\ u_{F_{c,y}} &= \tau_1(-m-3m_a)^{-1}z_v + \tau_1^{-1}F_{c,y} + \dot{F}_{c,y,des} - c_{F_{c,y}}z_{F_{c,y}} \end{aligned} \quad (28)$$

and the derivative of V_3 becomes

$$\dot{V}_3 = \dot{V}_2 - c_{F_{c,x}}z_{F_{c,x}}^2 - c_{F_{c,y}}z_{F_{c,y}}^2 \quad (29)$$

After the substitution of $u_{F_{c,x}}$ and $u_{F_{c,y}}$ in (25), the stabilized system is comprised by the subsystems (15), (24), and:

$$\begin{aligned} \dot{z}_{F_{c,x}} &= -c_{F_{c,x}}z_{F_{c,x}} - (1/(m-3m_a))z_u \\ \dot{z}_{F_{c,y}} &= -c_{F_{c,y}}z_{F_{c,y}} - (1/(m-3m_a))z_v \end{aligned} \quad (30)$$

4) Step 4

The next step is the stabilization of the subsystem (9b) to zero. The desired value for the virtual control r_e is (31) as it produces the stable equation (32).

$$r_{e,des} = -c_\psi \psi_e \quad (31)$$

$$\dot{\psi}_e = -c_\psi \psi_e \quad (32)$$

which drives ψ_e to zero. Following the same procedure as for x_e and y_e we compute the following control input for the stabilization of the orientation:

$$u_{N_{c,z}} = \tau_1(-m_{33}^{-1}z_r + (1/\tau_1)N_{c,z} + \dot{N}_{c,z,des} - c_{N_{c,z}}z_{N_{c,z}}) \quad (33)$$

The final Lyapunov function and the derivative are:

$$V_f = V_3 + (1/2)\psi_e^2 + (1/2)z_r^2 + (1/2)z_{N_{c,z}}^2 \quad (34)$$

$$\dot{V}_f = \dot{V}_3 - c_\psi \psi_e^2 - c_r z_r^2 - c_{N_{c,z}} z_{N_{c,z}}^2 \quad (35)$$

The final stabilized system is comprised by (15), (24), (30) and the equations produced from step 4:

$$\dot{\psi}_e = -c_\psi \psi_e + z_r \quad (36)$$

$$\dot{r}_e = (1/m_{33})n_z - \dot{r}_R + (1/m_{33})N_{c,z} \quad (37)$$

$$\dot{z}_{N_{c,z}} = -c_{N_{c,z}}z_{N_{c,z}} - (1/m_{33})z_r \quad (38)$$

Finally, we use the comparison lemma [9], to show that the errors defined by $\mathbf{w} = [x_e, y_e, \psi_e, z_u, z_v, z_r, z_{F_{c,x}}, z_{F_{c,y}}, z_{M_{c,z}}]^T$ will all converge to a neighborhood around zero. We consider $g = \min\{k, k_I, c_u, c_v, c_\psi, c_{F_{c,x}}, c_{F_{c,y}}, c_{M_{c,z}}\}$. It holds that:

$$\dot{V}_f \leq -2gV_f + (\|\delta\|^2/4k_1) \quad (39)$$

After the employment of the comparison lemma, we have:

$$V_f(t) \leq V_f(0)e^{-2gt} + (\|\delta\|^2/2g4k_1), \quad t \in [0, t_{final}) \quad (40)$$

and thus, we conclude that

$$\|\mathbf{w}(t)\| \leq \|\mathbf{w}(0)\|e^{-gt} + (\sqrt{\|\delta\|^2/g4k_1}), \quad t \in [0, t_{final}) \quad (41)$$

Error remains in a bounded set around zero.

C. The Stabilization Process - case B

In this section, we present the required formulations in order to design the control inputs when the dynamics of the forces/torque are approximated by a second order system (8d). We consider the following representation for the second order system (8d):

$${}^B \dot{\mathbf{t}}_c = \mathbf{p} \quad (42)$$

$$\dot{\mathbf{p}} = -(1/\tau_2)\mathbf{p} - (1/\tau_2){}^B \mathbf{t}_c - (1/\tau_2){}^B \mathbf{t}_{c,des}$$

where,

$$\mathbf{p} = [p_x, p_y, p_z]^T = [\dot{F}_{c,x}, \dot{F}_{c,y}, \dot{N}_{c,z}]^T$$

We continue the design of the backstepping controller from the forces' errors (23). From (42) we have:

$$\dot{z}_{F_{c,x}} = p_x - \dot{F}_{c,x,des} \quad (43)$$

We introduce the following Lyapunov function:

$$V_3 = V_2 + \frac{1}{2}z_{F_{c,x}}^2 \quad (44)$$

After, derivation of the Lyapunov function we compute $p_{x,des}$, so that all terms are negative except to $\|\delta\|^2/4k_I$:

$$p_{x,des} = \dot{F}_{c,x,des} - \frac{1}{m_{11}}z_u - c_{F_{c,x}}z_{F_{c,x}} \quad (45)$$

$$z_{p_x} = p_x - p_{x,des} \Rightarrow p_x = z_{p_x} + p_{x,des} \quad (46)$$

$$\dot{z}_{F_{c,x}} = -c_{F_{c,x}}z_{F_{c,x}} - \frac{1}{m_{11}}z_u + z_{p_x} \quad (47)$$

p_x is not a true control, so we have to introduce the error (46) and the substitution of (46) and (45) in (43) yields (47) which is part of the final stabilized system. The derivative of z_{p_x} is given from (42) and (46):

$$\dot{z}_{p_x} = -(1/\tau_2)p_x - (1/\tau_2)F_{c,x} - \dot{p}_{x,des} + (1/\tau_2)u_{F_{c,x}} \quad (48)$$

After augmenting the Lyapunov function with the half of the square of z_{p_x} and requiring all derivative terms to be negative except for $\|\delta\|^2/4k_I$, we compute the control $u_{F_{c,x}}$.

With the same methodology we can compute $u_{F_{c,y}}, u_{N_{c,z}}$:

$$\begin{aligned} u_{F_{c,x}} &= \tau_2(-z_{F_{c,x}} + \tau_2^{-1}p_x + \tau_2^{-1}F_{c,x} + \dot{p}_{x,des} - c_{p_x}z_{p_x}) \\ u_{F_{c,y}} &= \tau_2(-z_{F_{c,y}} + \tau_2^{-1}p_y + \tau_2^{-1}F_{c,y} + \dot{p}_{y,des} - c_{p_y}z_{p_y}) \\ u_{N_{c,z}} &= \tau_2(-z_{N_{c,z}} + \tau_2^{-1}p_z + \tau_2^{-1}N_{c,z} + \dot{p}_{z,des} - c_{p_z}z_{p_z}) \end{aligned} \quad (49)$$

The representation (42) can be inductively expanded, allowing the approximation of the forces/torque with even higher order systems. The three control inputs $u_{F_{c,x}}, u_{F_{c,y}}, u_{N_{c,z}}$ are directed to the allocation scheme, in the place of F_x, F_y, N_z , to be resolved into thrust and angle control inputs: $J_{a,des}, J_{b,des}, J_{c,des}$ and $\varphi_{a,des}, \varphi_{b,des}, \varphi_{c,des}$, respectively, see Fig. 3.

IV. THE THRUST UPPER LIMIT MANIPULATION HEURISTIC

In many over-actuated systems, see [12], [13], a model-based controller cancels the nonlinearities and a PID or a linear MPC handles the linear dynamics. The tuning is simple as we can handle the linear dynamics by adjusting the control gains. However, the platform is used to carry massive objects and the cancellation of mass terms reduces the performance of the controller. The backstepping controller, avoiding mass terms cancellation, increases system robustness. On the other hand, the gains in the backstepping controller cannot handle completely the evolution of the error variables of the stabilized system. For instance, equation (30) represents the

evolution of the force error variable. If the equation had the following form:

$$\dot{z}_{F_{c,x}} = -c_{F_{c,x}} z_{F_{c,x}} \quad (50)$$

the force error would converge exponentially to zero. Equation (30) consists of (50) augmented with the term $-(1/(m-3m_a))z_u$ which is not equal to zero due to: (a) the environmental disturbances, (b) the parasitic thrust, which is the undesired thrust produced while jet rotates from the current direction to the desired direction, and (c) the fact that the allocation scheme is a nonlinear, non “1-1” transformation. This extra term does not allow the force to converge to its desired value as the platform reaches its target. As a result, we observe saturation to the jets thrust. In the simulation environment, if we decrease the Thrust Upper Limit (TUL), the platform does not lose control; it exhibits larger displacements, due to disturbances. The idea is to gradually decrease the TUL and as a result the energy consumption.

The high energy requirements due to the full thrust, led to the introduction of TUL manipulation heuristic. In this heuristic, the TUL depends on the current distance d from the center of the circle targets. As the platform approaches the circle-target, the TUL is exponentially decreasing, and remains constant when the platform enters the target circle. The desired thrusts $J_{A,des}$, $J_{B,des}$, $J_{C,des}$, from the allocation scheme must not exceed this varying upper limit. The thrust upper limit $J_{max}=20\text{kN}$ is multiplied by a factor p which is described by the following relations,

$$p = \begin{cases} 1, & d \geq d_{init} \\ \exp((d - d_{init})/a), & d_{init} \geq d \geq r \\ \exp((r - d_{init})/a), & r \geq d \end{cases}$$

Where d_{init} is the initial distance from the center of the circle-target, r is the radius of the circle-target ($r = 5$ m), see Fig. 2. Using parameter a , we adjust the reduction of p . Parameter a must be tuned, so that the platform overcomes the disturbances without demonstrating weak positioning. Weak positioning corresponds to one of the following cases: (a) the platform does not enter permanently the circle, (b) oscillates around circle boundaries, and (c) diverges more than $2d_{init}$, before reaching the target.

If $J_{A,des}$, $J_{B,des}$, $J_{C,des}$ exceed the upper limit of $J_{max} * p$, we assign them the value of $J_{max} * p$ kN. Since $0 \leq p \leq 1$, the thrust constraint is always satisfied. Fig. 3 summarizes the implementation of the TUL heuristic.

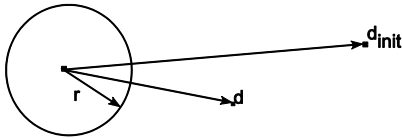


Figure 2. The circle-target.

V. SIMULATION RESULTS

A simulation example is presented. Our goal is to stabilize the position in a circle-target with center (0,0) and a radius ($r = 5$ m) and the direction at 0 deg., with tolerance ± 10 deg, under environmental disturbances, see Fig.4. Sensor noise

(± 1 m) is added to position and orientation readings. The initial values are: $x = -20.0$ m, $y = -20.0$ m, $\psi = -20.0$ deg, $u = 0.1$ m/s, $v = -0.1$ m/s, $r = -0.01$ rad/s.

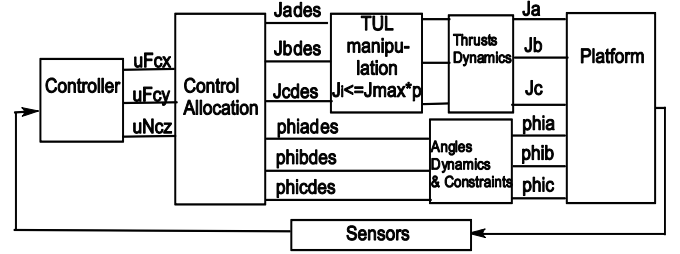


Figure 3. System Diagram.

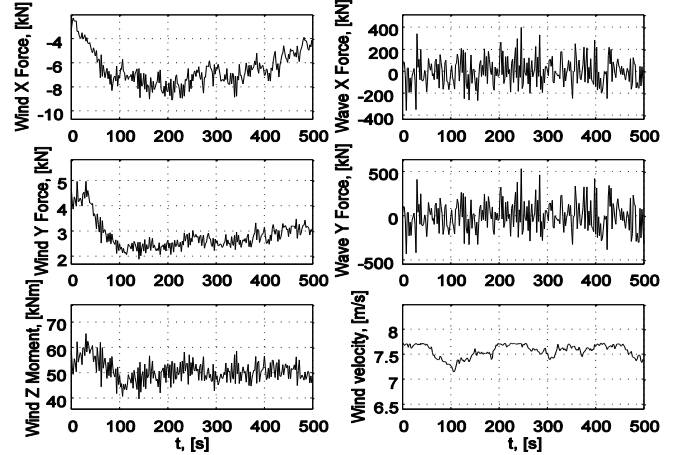


Figure 4. Environmental disturbances for the simulation run.

For **case A**: $k = 0.07$, $k_l = 0.07$, $c_u = 0.07$, $c_v = 0.07$, $c_{F_{cx}} = 0.07$, $c_{F_{cy}} = 0.07$, $c_\psi = 1.2$, $c_r = 0.7$, $c_{M_{cz}} = 0.7$. Parameter $a=143.72$ and when the CM of the platform enters the circle, $p=0.85$. For **case B**: $k = 0.5$, $k_l = 0.5$, $c_u = 2$, $c_v = 2$, $c_{F_{cx}} = 0.5$, $c_{F_{cy}} = 0.5$, $c_\psi = 4$, $c_r = 2$, $c_{M_{cz}} = 1$, $c_{px}=1$, $c_{py}=1$, $c_{pz}=1$. The parameter $a=45.58$, when the CM of the platform enters the circle, $p=0.4$. The p is tuned to reach the maximum possible reduction. Saturation limits are used to simulate the constraints. Thrust response without TUL manipulation (on the left) and with (on the right) are depicted in Fig. 5 for **case A**, and in Fig. 6 for **case B**. The TUL heuristic achieves greater reduction if it is applied when the dynamics of the forces/torque are approximated by a second order system.

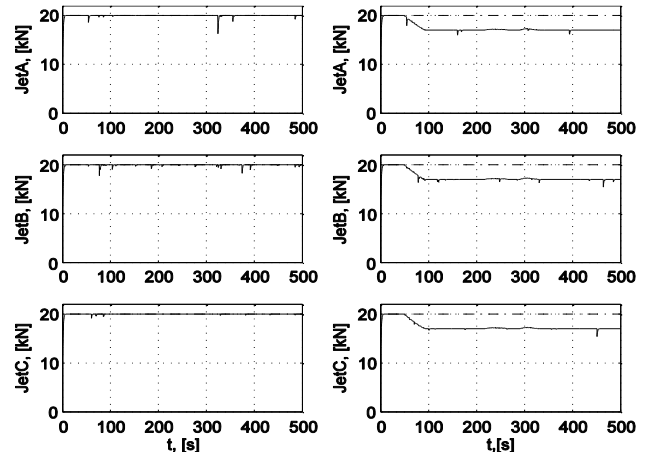


Figure 5. Case A, thrust: without heuristic (left), with heuristic (right).

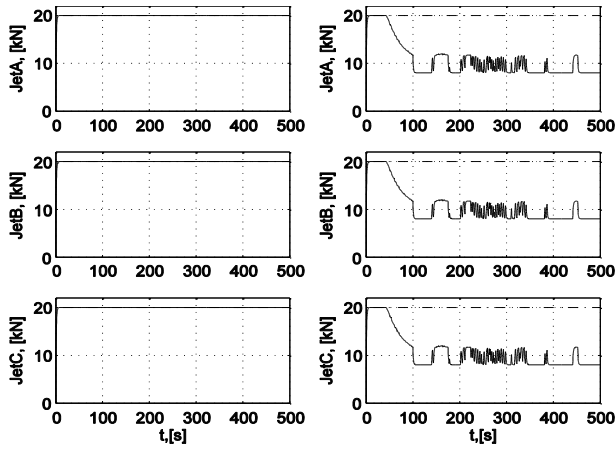


Figure 6. Case B thrust: without heuristic (left), with heuristic (right).

The 2D positioning is presented in Fig. 7, 8. The energy consumed by the platform, while accomplishing the task described in the simulation example, is summarized in Table I. In both cases, the introduced heuristic reduces the energy.

TABLE I. ENERGY CONSUMPTION

Energy consumed	without TUL manipulation	with TUL manipulation	percentage energy reduction
case A	1.28e+05	1.04e+05	-18.75%
case B	1.28e+05	5.18e+04	-59.53%

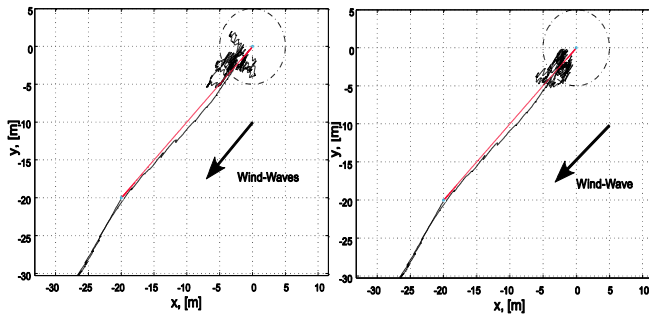


Figure 7. Case A: without heuristic (left), with heuristic (right).

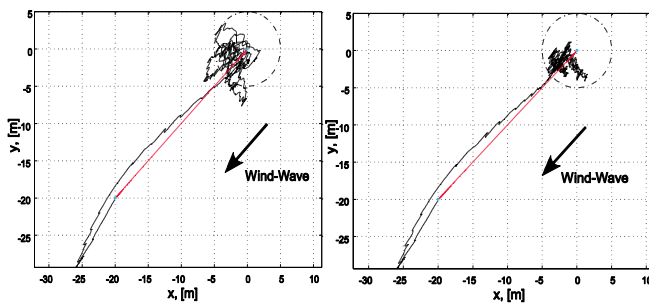


Figure 8. Case B: without heuristic (left), with heuristic (right).

In Table II, we compare controller robustness in the presence of mass estimation errors, while they accomplish the same task described in the simulation example. We record the max error in mass that the controller tolerates, while achieving the task of keeping the platform within the specified position, Fig. 7, 8. All versions of backstepping controller outperform the model-based, [12], [13], by 10-30% in mass error robustness.

TABLE II. ROBUSTNESS EXAMINATION

Controller	BS case A without TUL	BS case A with TUL	BS case B without TUL
max mass error(%)	-90%	-90%	-90%
Controller	BS case B with TUL	Model-based linear MPC	Model-based PID
max mass error(%)	-90%	-80%	-60%

VI. CONCLUSION

We presented the design of a backstepping controller aiming at the dynamic positioning of an overactuated marine platform. The settling delays, the dynamics of the thrusts and the angles and hardware limitations have been taken into account. The asymptotic stability of the controller was established, and simulation results illustrated its performance, under realistic environmental disturbances. Simulation results showed that the TUL heuristic reduces the thrust requirements and the energy consumed.

REFERENCES

- [1] www.nestor.noa.gr
- [2] Sørensen, A.J., "A Survey of Dynamic Positioning Control Systems," in *Annual Reviews in Control*, vol. 35, no. 1, April 2011.
- [3] Wilson, J. F., *Dynamics of Offshore Structures*, New Jersey, John Wiley and Sons, 2003.
- [4] Thor I. Fossen, *Handbook of Marine Craft Hydrodynamics and Motion Control*, First Edition, 2011, John Wiley & Sons Ltd.
- [5] Johansen, T. A., and Fossen, T. I. (2013). Control allocation—a survey. *Automatica*, 49(5), 1087-1103.
- [6] Witkowska, A., and Smierzchalski, R., "Nonlinear Backstepping Ship Course Controller," *International Journal of Automation and Computing*, 2009, 6(3), pp. 277-284.
- [7] Lin Xiao, Jouffroy, J., "Modeling and Nonlinear Heading Control of Sailing Yachts", *IEEE Journal of Ocean Engineering*, Volume:39, Issue: 2, Publication Year: 2014, Page(s): 256-268.
- [8] Ghommam, J., Mnif, F., Benali, A., Derbel, N., "Asymptotic Backstepping Stabilization of an Underactuated Surface Vessel", *IEEE Transactions on Control Systems Technology*, Volume: 14, Issue: 6, Publication Year: 2006, Pages(s): 1150-1157.
- [9] Repoulia, F. and Papadopoulos, E., "Planar Trajectory Planning and Tracking Control Design for Underactuated AUVs," *Ocean Engineering*, Volume 34, No. 11-12, August 2007, pp 1650-1667.
- [10] Bateman, A., Hull, J., Zongli Lin, "On the Properties of the Backstepping Design for Marine Vehicles," *33rd Annual Conference of the IEEE Industrial Electronics Society 2007*, vol., no. 5-8, pp. 504,509.
- [11] Feemster, M. G. and Esposito, J. M. (2011), "Comprehensive framework for tracking control and thrust allocation for a highly overactuated autonomous surface vessel," *J. Field Robotics*, 28: 80-100. doi: 10.1002/rob.20369.
- [12] Vlachos, K.; Papadopoulos, E., "Control design and allocation of an over-actuated triangular floating platform," *2010 IEEE International Conference on Robotics and Automation (ICRA)*, 3-7 May 2010.
- [13] Tsopelekos A., Vlachos K., Papadopoulos E., "Design of a Linear Model Predictive Controller for an Overactuated Triangular Floating Platform," *Proc. 2014 IEEE Multi-conference on Systems and Control*, Antibes, France, October 8-10, 2014.
- [14] Naghshineh, Mehrdad, and Mehdi Keshmiri, "Actuator saturation avoidance in overactuated systems," *Proceedings IEEE/RSJ International Conference on Robots and Systems (IROS 2004)*, Vol. 4. IEEE, 2004.
- [15] Khalil, H. K., *Nonlinear Systems*, second ed. Prentice-Hall, Upper, Saddle River, 2002.